HHS Public Access

Author manuscript

Min Metall Explor. Author manuscript; available in PMC 2022 July 13.

Published in final edited form as:

Min Metall Explor. 2021 ; 38(2): 885–896. doi:10.1007/s42461-020-00369-5.

Moderate Cover Bleeder Entry and Standing Support Performance in a Longwall Mine: a Case Study

Mark Alexander Van Dyke[1], **Ted M. Klemetti**[1], **Ihsan Berk Tulu**[2], **Deniz Tuncay**[2]

[1]Ground Control Branch, CDC NIOSH, Pittsburgh Mining Research Division, Pittsburgh, PA 15236, USA

[2]Mining Engineering Department, West Virginia University, Morgantown, WV 26505, USA

Abstract

Bleeder entries are critically important to longwall mining for the moving of supplies, personnel, and the dilution of mine air contaminants. By design, these entries must stay open for many years for ventilation. Standing supports in moderate cover bleeder entries were observed, numerically modeled, and instrumented by researchers at the National Institute for Occupational Safety and Health (NIOSH). The measurements of the installed borehole pressure cells (BPCs), standing support load cells and convergence meters, and roof extensometers are presented in this paper in addition to the numerical modeling results and visual observations made by the NIOSH researchers in the bleeder entries. The results include the effects of multiple panels being extracted in close proximity to the instrumented site as well as over one and a half years of aging. As expected, standing supports closer to the longwall gob showed the greatest load and convergence. The roof sag appeared generally independent of the proximity to the longwall gob. The BPC readings were driven by both the proximity to the gob and the depth into the pillar. The results of this study demonstrated that the entry roof can respond independently of the pillar and standing support loading. In addition, the rear abutment stress experienced by this bleeder entry design was minimal. The closer the mine development, pillar, or supports are to the gob, the greater the applied load due to rear abutment stress.

Keywords

Longwall mining; Geology; Bleeders; Support

✉Mark Alexander Van Dyke, mvandyke@cdc.gov.

Authors' Contributions All authors contributed to the draft of the manuscript. Material preparation, installation, and data collection were performed by Mark Van Dyke and Ted Klemetti. Modeling was performed by Berk Tulu and Deniz Tuncay. All authors read and approved the final manuscript.

Conflict of Interest The authors declare that they have no conflict of interest.

Publisher's Disclaimer: Disclaimer The findings and conclusions in this report are those of the author(s) and do not necessarily represent the official position of the National Institute for Occupational Safety and Health (NIOSH), Centers for Disease Control and Prevention. Mention of any company or product does not constitute endorsement by NIOSH.

1 Introduction

In retreat longwall mining practice in the USA, the bleeders are used to ventilate the gob areas of the active mining district. Air passing through the gob and bleeders will continuously dilute the methane, dust, and other contaminants released after mining. Typically, the bleeders will consist of multiple bleeder systems from adjacent longwall panels within a district. The number of longwall panels in a district depends on many factors such as ventilation, geology, and property boundaries, but typically there are 4 to 5 longwall panels in a district.

The condition of longwall bleeder entries depends on factors such as local geologic conditions, overburden, age, and stress redistribution of the rear abutment stress as the longwall retreats. This paper will focus on the redistribution of stress of the bleeder entries and pillars over a 550-day period during mining longwall panel of the instrumented bleeders and the adjacent longwall. Figure 1 shows a typical bleeder, gateroad, and longwall panel.

The National Institute for Occupational Safety and Health (NIOSH) has continued a research effort to better understand the performance of standing supports in bleeder entries in longwall mines in different conditions. Previous studies performed by Klemetti et al. [1, 2] suggested that the installed standing supports that were monitored were never exposed to stresses that came close to their maximum capacity. Entry convergence was very minor, and the rear abutment stress caused very little change to the stability of the bleeder systems even after multiple panels were mined in deep overburden in the Pocahontas seam and non-typical bleeder systems in the Blue Creek and Mary Lee seams. The question NIOSH researchers were determined to answer is how do these two bleeder support scenarios compare to a typical bleeder design in moderate overburden in the Pittsburgh coal seam?

2 Mine Layout

The mine in this study is located on the border between North Central West Virginia and Southwestern Pennsylvania, mining the Pittsburgh coal bed. The mine utilizes the longwall mining technique with a three-entry gateroad system. The geometric layout of the mine and study area can be seen in Fig. 2. The depth of cover at this mine ranges from 122 to about 427 m. The longwall panels, in close proximity to the study site, are 335 m wide and are 3600 m long. The gateroad consists of a small and a large pillar with center to center dimensions of 27.5 by 42.7 and 50.3 by 85.3 m, respectively. The entry and crosscuts in the gateroads are 5.5 m wide and range between 1.8 and 3.7 m in height. The bleeder entries are developed at the startup side of the longwall panel. There are four entries including the startup room. The three pillars separating the four entries are 30.5, 39.6, and 19.8 m and between 57.9 and 91.4 m long with the longer pillars being the widest pillars. The entry dimensions in the bleeders are the same as those in the gateroads.

The installed support in the study area consists of 2.44-m fully grouted rebar bolts on a 1.22 by 1.22-m spacing. The fully grouted bolts are supplemented with 3.66-m cable bolts in the intersections. There are six cable bolts per intersection. In addition, standing supports are installed in the gateroads and bleeders. The typical standing support is a 68.6-cm pumpable

crib when the mining height is less than 2.44 m and a 76.2-cm pumpable crib when higher. These standing supports use patterns of six per intersection, a single row spaced 2.44-m skin-to-skin, a double row spaced 2.44 m skin-to-skin, and various other spacing depending on depth of cover, distance to longwall gob, and importance of the entry.

3 Geologic Setting

The Pittsburgh coal seam was deposited during the late Pennsylvanian period in areas of Pennsylvania, West Virginia, Ohio, and Maryland. The gently dipping basin was being filled by sediments from mountainous regions to the east. The Pittsburgh coal bed is in the Monongahela Group which consists of cyclothem sequences of limestones, coals, shales, and sandstones. The sediments deposited varied depending on the transgression and regression of sea levels (see Fig. 3). The Pittsburgh basin deposits contain large sandstone and limestone deposits depending on and upper or lower delta region. The upper delta region is dominated by massive sandstone roof lithology that trends to the far east and western sides of the basin. The middle of the basin is dominated by fresh water limestone deposits of the lower delta [3].

The area of the instrumentation site was located near a transition zone from a limestone-dominated roof to sandstone lithology. The lithology consists of thinly bedded to laminated shales and sandstones which provide generally weak roof conditions that delaminate under high stress conditions. The closest corehole (see Fig. 4) to the study site contains a combined 2.29 m of Pittsburgh coal bed main bench, claystone (draw slate), and roof coals. Above the roof coal are 6.07 m of sandy shales and sandstones which make the bolted horizon. After the sandstone, a 22.4-m sequence of limestone and shales form the remainder of the immediate roof strata. The floor consists of 0.87 m of shale immediately below the main bench followed by 13.16 m of interbedded limestones and shales.

4 Field Mapping

Field mapping was performed five times throughout the study to assess the geology and performance of the entries and supports during the duration of the study. A rating system of 0–5 for the roof, ribs, and floor was chosen based on previous work described in Klemetti et al. (see Fig. 5), which reflects previous methods used in the past [5, 6].

The conditions of the floor, roof, and ribs were observed at a minimum in every crosscut, and once in the straight between the crosscuts. The first mapping occurred before the mining of the longwall panel 4. The last mapping was performed when the longwall was near the completion of the panel. The ratings for the first and last mapping can be compared in Fig. 6.

Overall, conditions were stable over the duration of the study. The entry with the most damage was the foreman’s entry which is the closest bleeder entry that was accessible after the longwall started. The center of the foreman’s entry towards the center of the panel and the gateroads leading to the bleeders and longwall face had a change in the entry rating while the rest of the bleeder system remained consistent.

5 Instrumentation

The study area was chosen to be in the bleeders of panel 4. The average depth of cover was approximately 283.5–289.6 m in the three bleeder entries. The average dimensions of the entries were 2.29 m long and 4.88 m wide. The pillar dimensions are 61 m by 30.5 m and 39.6 m center to center. The instrumentation in the study area included borehole pressure cells (BPC), 4-point roof extensometers (4-pt RE, and standing support load cells (SSLC), and convergence meters (SSCM) as seen in Fig. 7. The BPC and 4-pt RE were installed while the bleeder entries were being developed. This meant that the previous panel, panel 3, was finishing the retreating of the panel and changes in abutment loading from panel 3 would not be measured. The SSLC and SSCM were installed when the standing supports were installed. These supports were installed after the development of the bleeder entries and just prior to the beginning of the retreat of panel 4.

There are four smaller sites within the larger study area that monitored the standing supports. The first site is furthest from the startup room (96 m away) in a 3-way intersection, the second is 24.4 m closer to the startup room (71.6 m away) in a 4-way intersection, the third is in a 3-way intersection in the entry immediately behind the startup room (30.5 m away), and the fourth is in the 2nd entry behind the startup room adjacent to the second site. The four sites were chosen to investigate the rear abutment extent and loading as well as difference between entry, 3-way intersection, and 4-way intersection loading. Each of these four sites has two pumpable cribs with SSLC and SSCM and one pumpable crib with only a SSLC. Sites one, two, and three also have a 4-point RE with anchor horizons at 6.1, 4.9, 3.7, and 2.4 m. There are five BPCs installed into the three pillars in the bleeder entry area. BPC 5 is installed in the pillar immediately behind the startup room (18.3 m away); BPC 3, 4, and 2 are installed in the second pillar behind the startup room (39.6, 48.8, and 59.4 m away); while BPC 1 is installed in the pillar furthest from the startup room (82.3 m away).

The results of the instrumentation study can be divided into three areas: (1) pillar loading, (2) roof deformation, and (3) standing support response. Area 1, pillar loading, includes the BPC measurements from the five locations (Fig. 8), and the measured load can be seen in the figure. The pillar loading was not recorded during the first few feet of advance of panel 4; however, the initial load was measured, allowing for a change in load to be determined for the first 609.6 m of panel 4 extraction. BPCs 3 and 5 showed the greatest increase in load due to the first 609.6 m of panel 4 retreating. These two BPCs showed approximately 3.44 MPa increase in load. BPC 3 showed a continued increase to a total of about 6.88 MPa before dropping back to the 3.44 MPa increase after the first 609.6 m. BPC 5 showed a slight decline for about the next 8 months, then an increase of 1.38 MPa. BPCs 1, 2, and 4 showed little to no change due to the first 609.6 m of panel 4 retreating. If anything, they all showed a slight decrease in load. BPC 2 did not record data for a month and a half due to a dead battery. BPC 2 also quit reading in May 2019 about 3 months after panel 5 began retreating. BPC 3 showed a large load decrease during the mining of panel 4, which may be due to localized failure of the borehole in which the cell is located, local redistribution of load, or possibly a data logger issue.

The second measurement data set includes the roof extensometers for the three sites. Figure 9 shows the roof sag for the three intersections monitored. The intersection closest to panel 4 gob shows the largest roof sag of 1.5 mm at the roof line after the first 609.6 m of panel 4 is retreated. The same roof extensometer peaks at 7.9 mm at the roof line after the first 609.6 m of panel 5 is retreated. The other two intersections further from the startup room of panel 4 show essentially no roof sag to date—panel 4 is complete, and Panel 5 is nearly complete. Aside from the increases seen in the intersection nearest the startup room, the roof extensometers did not show a noticeable difference due to proximity to the startup room or gob nor did it show any difference between 3-way and 4-way intersections.

The final measurement data set includes the convergence and loading measured on standing supports in the bleeder entries. A total of eight standing support convergence meters were initially installed, and within 45 days, there were only five that survived the startup of longwall panel 4. The resulting convergence for these five meters can be seen in Fig. 10. The convergence did not show significant movement during panel 4 retreating, less than 4.22 mm, nor did it show much more movement due to panel 5 retreating, less than an additional 2.22 mm. These results by themselves would lead to a belief that the standing supports are not required to resist much movement. To supplement the limited convergence data and evaluate the standing supports a little more, load cells were placed on the bottom of 12 standing supports located in the four sites as shown in Fig. 7.

The load cell measurements can be seen in Fig. 11. The first interesting result of the standing support load cell measurements is the fact that many of the cells did not record pressure continuously throughout the entire study period. Several of the load cells stopped recording data shortly after panel 4 squared up or retreated and passed the 609.6-m mark. Two of the four load cells began reading 1 month before panel 5 startup. Three other load cells quit recording between 1 and 2 months prior to panel 5 startup. At the last download, seven cells were still recording. At the startup and through the squaring of panel 4, all of the standing support load cells were recording and the average increase was about 618 kN, with a peak of 820 kN and a minimum of 140 kN. These readings are well below the 1800-kN capacity of the pumpable cribs monitored. The measured load continued to increase during the remainder of panel 4 retreat, not due to abutment loading. During panel 5 startup, through squaring at 609.6 m of retreat, there were six cells still recording data. The remaining six cells showed an average increase of 60 kN during this period with a minimum of 4.4 kN and a maximum of 133 kN. The load cells and convergence measurements were realistic when compared to the results from laboratory testing in the mine roof simulator [7].

6 Numerical Modeling

In an attempt to understand the loading mechanism of bleeder entry system, a large-scale 3D model of the mine is analyzed. A recently developed numerical modeling approach is applied to the case study mine [8]. A FLAC3D model was developed to replicate the geometric and geologic setting of the study site with a focus on the instrumentation locations at the actual study site. The overburden in the study area consists of alternating layers of sandy shale, sandstone, fireclay, and coal. Interfaces between the geological layers in the overburden were modeled with interface elements. Coulomb’s criterion was used to define

the limiting shear strength of the interfaces. As described by Su, the coefficient of friction of interfaces was set to 0.25, which is an approach he successfully applied to various longwall mine cases for estimating subsidence and pillar stresses [9, 10].

In developing the FLAC3D panel scale model, first, a 2D model was developed employing actual stratigraphy, using all the geological layers from a nearby corehole with a minimum modeled layer thickness of 0.5 m. The main purpose the 2D model is to verify the material properties assigned to different overburden layers prior to the 3D model. The 2D model of the mine had 87 different overburden layers with thicknesses ranging from 0.5 to 25.9 m to simulate the overburden. The 2D model results were compared with the VPI empirical subsidence prediction program, the surface deformation prediction system (SDPS) [11, 12]. The FLAC model approximated subsidence of the panel with average overburden depth of 290 m, panel width of 305 m, and hard-rock ratio of 25% within 5% of the SDPS prediction. The 2D model had approximately 1.2 million elements. In order to generate a 3D model that can run in a reasonable time frame, the minimum thickness of overburden layers is increased to 4.0 m. In order to generate a 3D model that can approximate stresses accurately with larger elements, overburden lithological layers with the same rock type with thickness less than 4.0 m were combined and represented with a transversely isotropic elastic material model. The element size of the overburden layers gradually increases along the ± z-direction, most detailed gridding being at the instrumentation site with 1-m elements. The 3D model of the mine had 24 different overburden layers and approximately 1.1 million elements in total. The coal model and material properties are those previously developed by NIOSH researchers to produce correct dilation, peak strength, and residual strength responses while still conforming to the Bieniawski pillar strength formula [8]. The stability mapping grid generator developed for the LaModel stress analysis software is used to generate the mine layout at the seam level [13]. The instrumented pillars, roof, and floor were simulated with 1.0-m elements as seen in the plan view (see Fig. 12). The figure shows two stages of increasing zone density, the most detailed area (1.0-m elements) centered on the instrumented pillars. The second stage encapsulating the entire study area with element sizes of 2.5 m. The remaining elements of the seam layer are 5.0-m elements. The geometry of the model with the representative geological sequence that was modeled is shown in Fig. 13.

6.1 Numerical Modeling Results

The numerical model was solved in five stages, the first being development. The second and third steps are the complete retreating of the second and third panels of the current district. The fourth stage is the first 100 m of the fourth panel extracted, which is followed by the fifth stage being the complete retreat of the fourth panel. The primary modeling results of interest to this study are that of the stress redistribution and rib yielding depth due to longwall extraction. The global stress redistribution due to the five evaluation steps of the numerical model can be seen in Fig. 14.

The entries mined for the development stage, step 1, produce an increase in the stresses near the entries. The majority of the stress changes for the panel retreating are localized to the gateroads and other nearby solid coal elements. To better see the changes in the stresses in

the study area, a local stress plot is shown in Fig. 15. The instrumented area only shows minor increases during the first three steps. With the start of the third panel retreat, the instrumentation area starts to show stress changes on the pillars closest to the gob. The row of pillars adjacent to the gob shows peak or near peak stress deep into the pillar corners closest to the gob. Based on observed rib conditions, the modeled depth of pillar yielding and peak loading appears reasonable. However, since the ribs showing these loads are in the startup room, observations of the conditions cannot be made once the longwall starts retreating.

The model results for the specific locations of the installed BPC can be seen in Table 1. The modeled results for the 5 BPC installed showed no change in load during the first three steps of the model, which were associated with the development and retreating of the two previous panels.

Table 2 shows the comparison between the modeled and measured stress changes for BPC-3 and BPC-5, where stress increase was recorded by the BPCs. The BPC closest to the gob (BPC-5) showed a large increase due to the first 100 m of panel 4 being retreated (step 4) and upon completion of the mining of panel 4 (step 5), much higher than what the measurements indicate. Compared to the field measurements, the model showed similar results for BPC-3 with an increase of 2.2 MPa within the first 100 m and going as high as 5.4 MPa with the completion of panel 4.

Another view of the modeling vertical stress results is the cross-section from instrumentation site to panel 4 gob (A-A') for each of the 5 modeling steps shown in Fig. 16. There is almost no change in stress during the development and the complete retreat of the first two panels. Figure 15 shows a large peak stress in the barrier pillars with a rapid decay as the distance to the gob increases. The BPCs show a similar response in that the BPCs closest to the gob show the greatest increase in stress, while those farthest away show no increase in stress. Likewise, the visual observations agree with the stresses being greatest when closest to the gob and decreasing as the distance increases, especially for the rib conditions.

7 Conclusions

The study site was performed under typical mining conditions for longwall mines in the Pittsburgh seam. The roof lithology consisted of thinly bedded to laminated shales and sandstones. The longwall panel dimensions were 335 m wide and 3600 m long with overburden depths at approximately 289.6 m. All of these conditions are what the majority of Pittsburgh seam longwall mines typically encounter.

Based on observations, the most critical steps to maintaining bleeder entries beyond the initial installed support is to focus on skin control of the roof. The majority of stress-related entry damage occurred in the center of the panel in the first entry of the bleeder. Otherwise, most damage visually noted was due to the sag of the first 0.15 m of roof that occurred over time.

The installed instrumentation suggested that the bleeders were over supported. The BPCs showed a 3.44–6.88 MPa increase during the time monitoring the mining of two longwalls,

which is low enough to support the notion that the bleeders are over supported. The roof extensometer measured a minimal amount of roof sag of less than 0.9 cm, which is less than the 30-mm limit often used in Australian TARPS [14] and the 25 mm observed in two Pittsburgh seam mines without failure [15]. The load and convergence experienced by the standing supports were significantly less than the 5.08 to 10.16 cm of movement suggested before pumpable cribs are required. The modeled results also suggest that stress levels experienced on the pillars and entries of the bleeders are slightly increased throughout the extraction of the first and second longwall panels. These results are very consistent with the previous studies performed by Klemetti et al. [1, 2].

Numerical modeling of the scenario suggests that there is some additional stress exerted on the bleeder pillars and entries in this study. Table 1 shows a much larger increase in stress between mining steps 3–4 and 4–5 than was measured by the BPC. However, the visual observations and the instrumentation results support that the entries with the current design and support are adequate for safe usage for ventilation and personnel passage.

References

1. Klemetti Ted M., Van Dyke Mark A., and Tulu Ihsan B. (2017). “Deep cover bleeder entry performance and support loading: a case study,” Proceedings of the 36th International Conference on Ground Control in Mining, July 26–28, pp. 208–219
2. Klemetti Ted, Van Dyke Mark, Tulu Ihsan B., and Tuncay Deniz (2019a). “A case study of the stability of a non-typical bleeder entry system at a U.S. Longwall Mine,” Proceedings of the 38th International Conference on Ground Control in Mining, July 23–25, pp. 267–275
3. Tewalt Susan J., Leslie Ruppert F., Bragg Linda J., Carlton Richard W., Brezinski David K., Wallack Rachel N., and Butler David T. (2000). “A digital resource model of the upper Pennsylvanian Pittsburgh coal bed, Monongahela Group, north Appalachian basin coal region”, Professional Paper 1625-C, U.S. Geological Survey
4. Klemetti TM, Van Dyke MA, Compton CS, Tulu IB, Tuncay D, and Wickline J (2019b). “Longwall gateroad yield pillar response and model verification – a case study,” The American Rock Mechanics Association 53rd U.S. Rock Mechanics/Geomechanics Symposium, June 23–26
5. Mucho TP, and Mark C (1994), “Determining horizontal stress mapping technique,” Proceedings of the 13th International Conference on Ground Control in Mining, August 2–4, pp. 277–289
6. Shepherd J, Humphreys DR, Rixon LK, and Creasey JW (1984). “Geotechnical investigations of roadway rib instabilities during mine development at Harrow Creek Trial Colliery, Queensland. Proceedings of the 5th Australian Tunneling Conference, Vol.5 Sydney, NSW Australia: Institution of Engineers, Australia, pp. 186–191
7. Barczak TM and Tadolini SC (2008). “Pumpable roof supports: an evolution in longwall roof support technology”. 2008 SME annual meeting and exhibit. Denver, CO: Society for Mining, Metallurgy, & Exploration, SME Preprint 08–034
8. Tulu IB, Esterhuizen GS, Gearhart DF, Klemetti TM, Mohamed KM, and Su DWH (2017). “Analysis of global and local stress changes in a longwall gateroad.” In: Proceedings of the 36th International Conference on Ground Control in Mining. Morgantown, WV: West Virginia University, July 26–28, pp. 100–110
9. Su DWH (1991). Finite element modeling of subsidence induced by underground coal mining: the influence of material nonlinearity and shearing along existing planes of weakness. In: Peng SS, editor. Proceedings of the 10th International Conference on Ground Control in Mining. Morgantown, WV: West Virginia University; June 10–12, pp. 287–300
10. Su DWH (2016). Personal communication
11. Agioutantis Z, Karmis M (2017) Quick reference guide and working examples. SDPS for Windows, Version 6:2J

12. Karmis M, Jarosz A, Agioutantis Z (1989) Predicting subsidence with a computer. Coal 26(12):54–61

13. Wang Q, and Heasley K 2005. Stability mapping system. In: Proceedings of the 24th International Conference on Ground Control in Mining, Morgantown, WV: West Virginia University, august 2–4 pp. 243–249

14. NSW code of practice, (2017). Strata control in underground coal mines. http://www.resourcesandenergy.nsw.gov.au/__data/assets/pdf_file/0003/543945/NSW-code-of-practice-Strata-control-inundergound-coal-mines.pdf

15. Chen J, Beck K, Bower J, Mishra M, Barczak T, and Huff C (2003). “Design considerations of the secondary roof support for longwall tailgate entries”, Proceedings of the 22nd International Conference on Ground Control in Mining, August 3–5, pp. 294–299

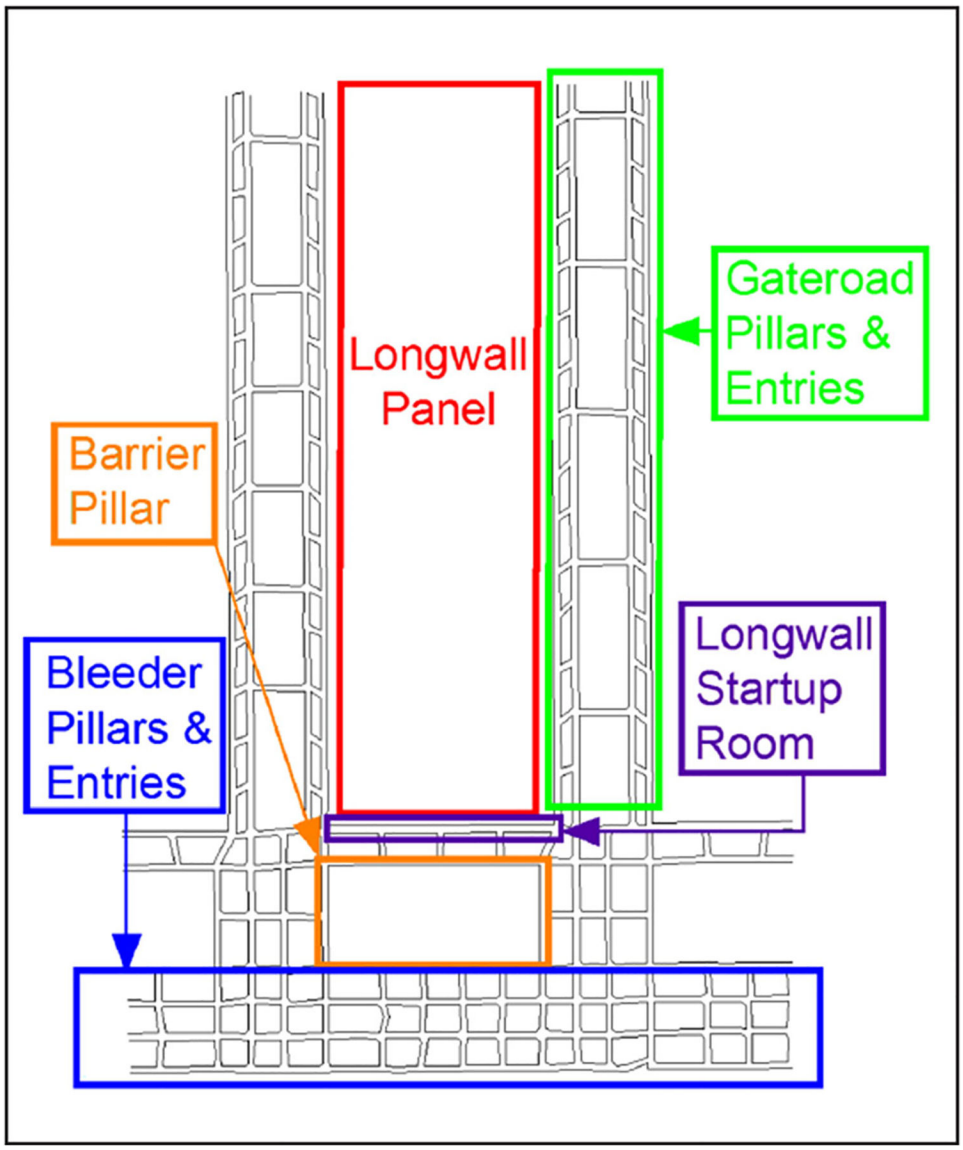

Fig. 1.
Generalized layout of the startup area of a longwall panel showing the location of the bleeder entries [1]

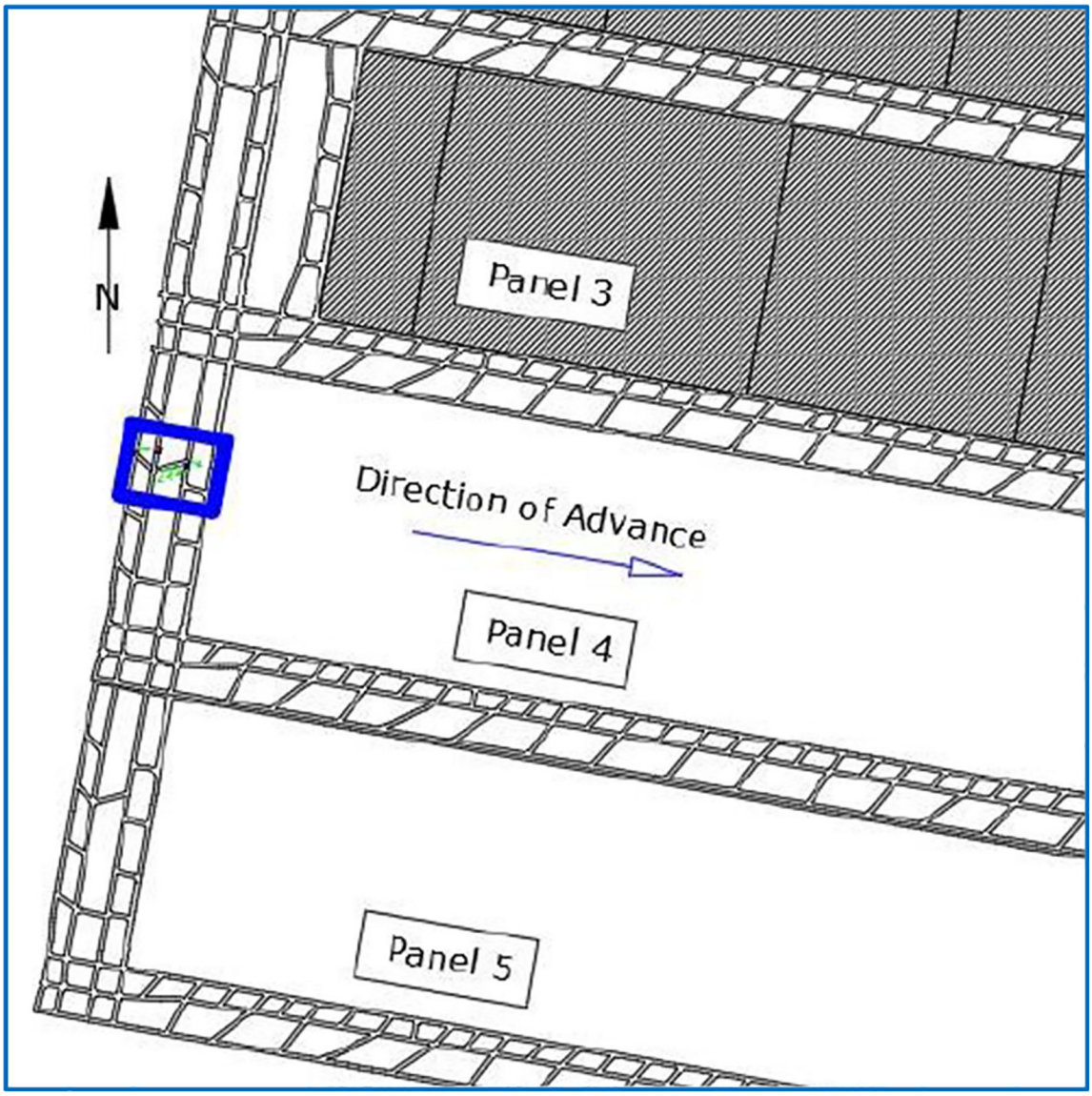

Fig. 2.
Overall mine geometry with the study area highlighted

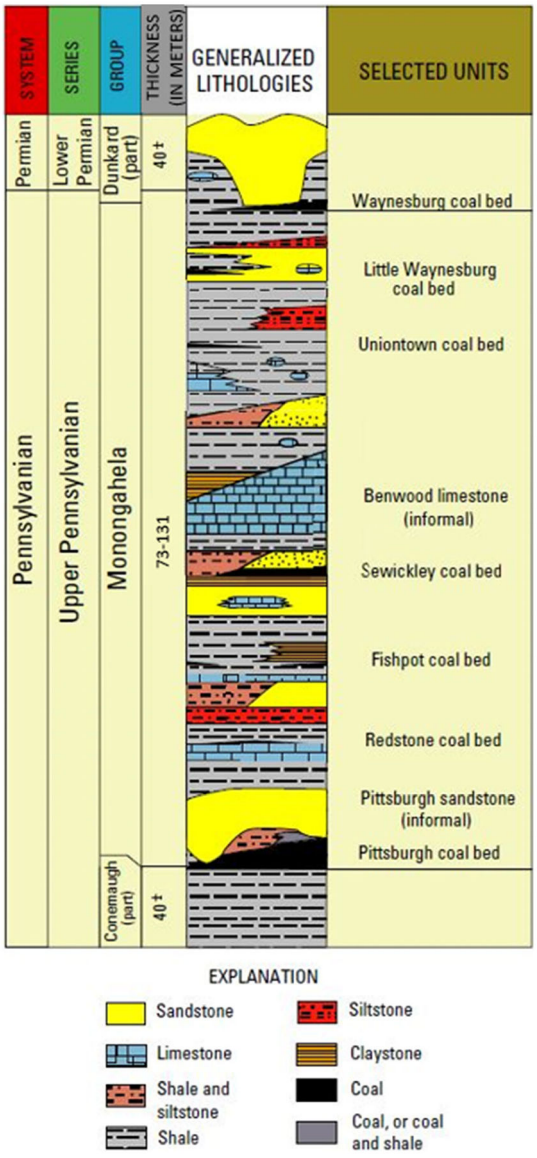

Fig. 3.

General stratigraphic column of the Monongahela group including the Pittsburgh seam [3]

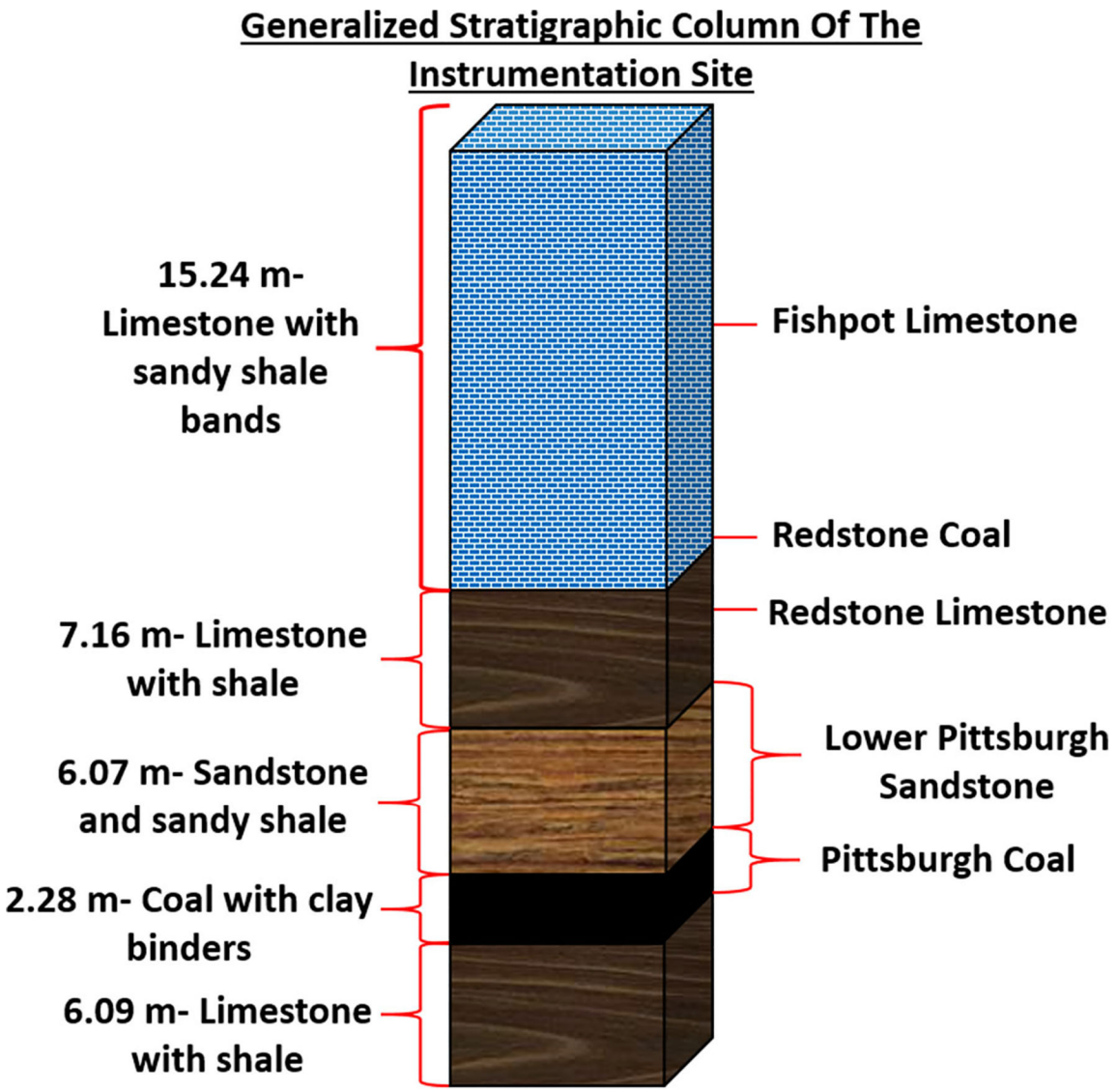

Fig. 4.
Generalized stratigraphic column of the study site

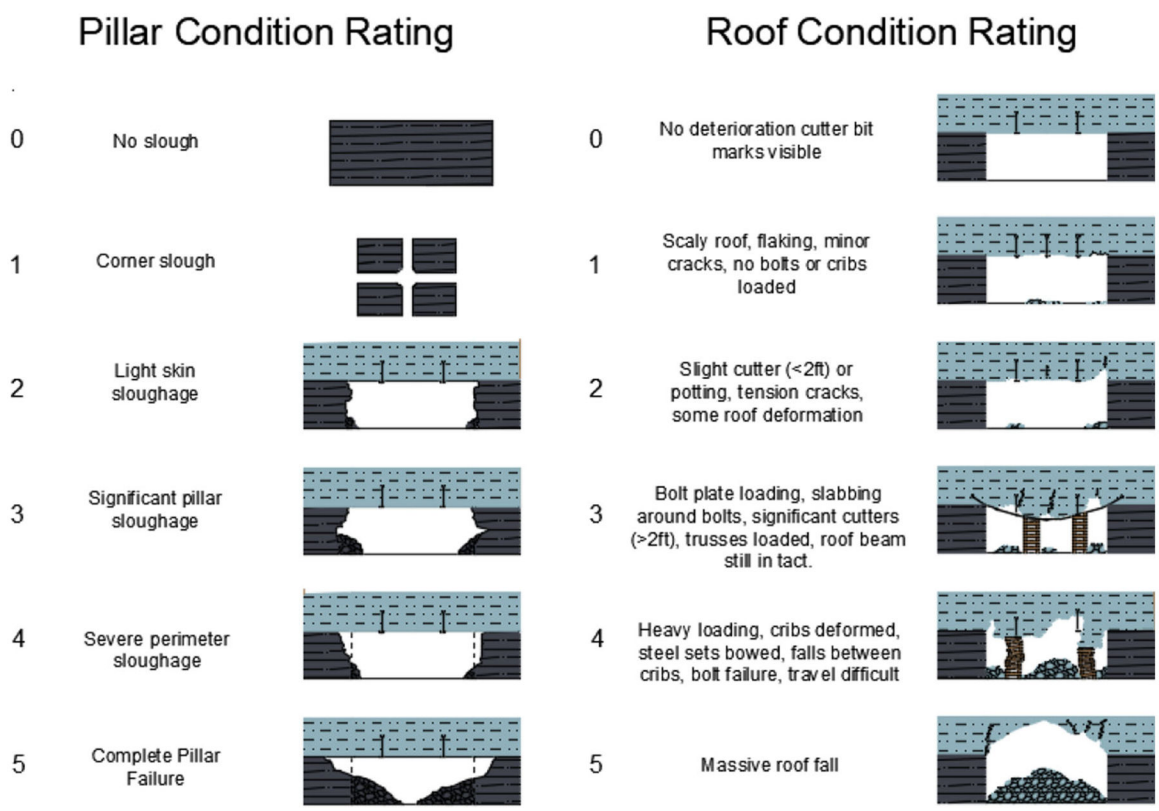

Fig. 5.
Roof and pillar rating system used for the condition mapping [4]

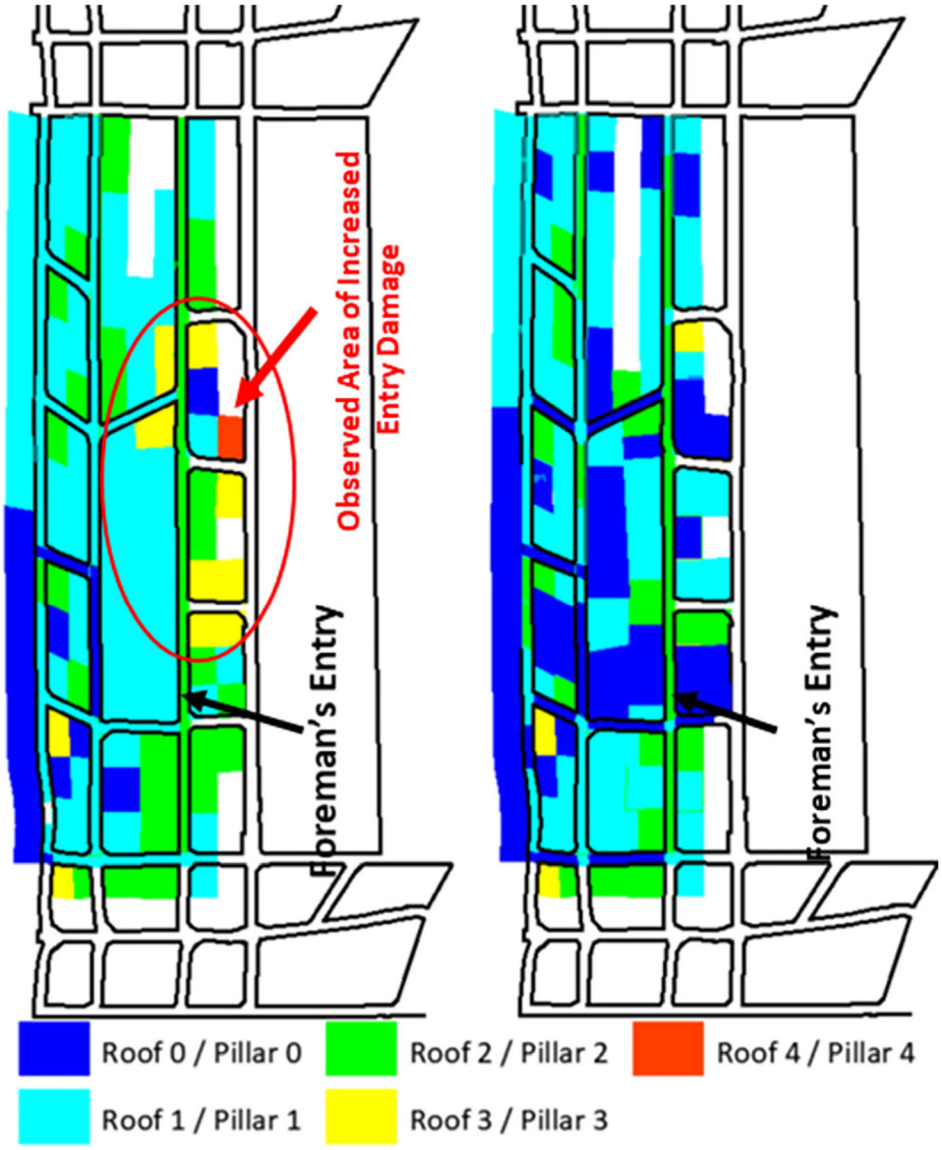

Fig. 6.

Condition mapping for the studied bleeder. The left is the final mapping and the right is the initial mapping

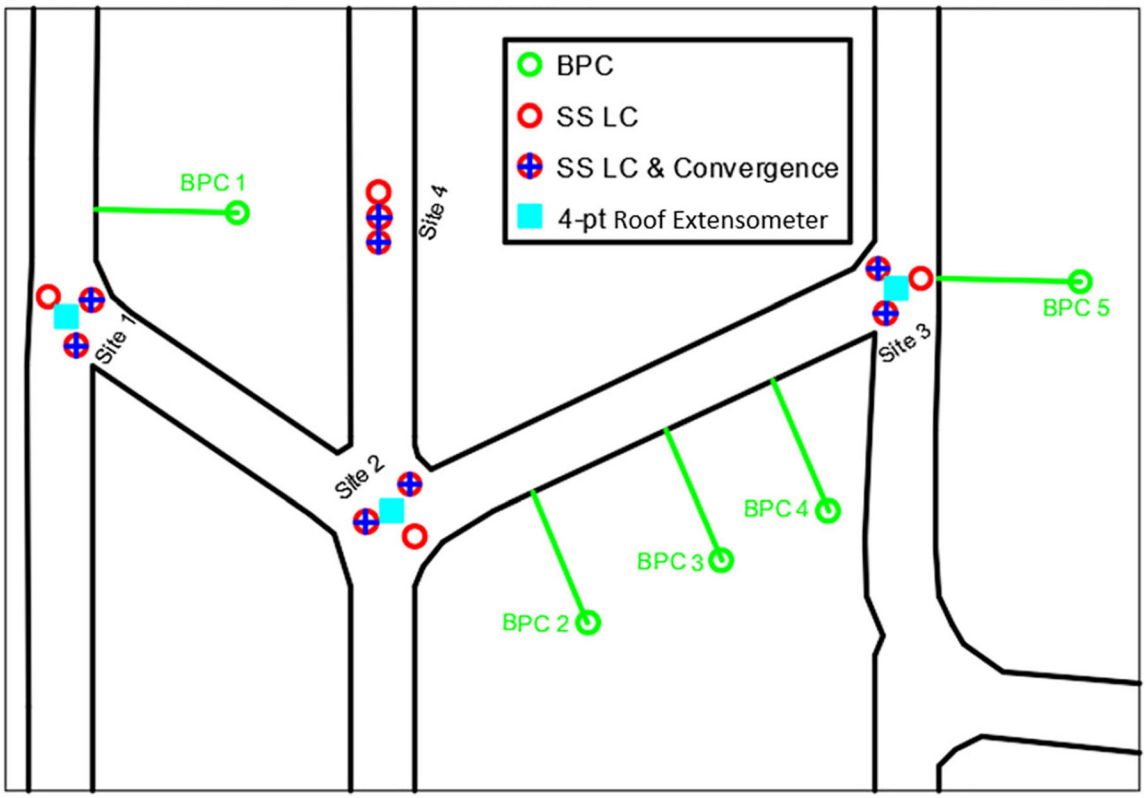

Fig. 7.

Instrumentation layout as installed; showing BPCs, standing support load cells and convergence meters, and 4-pt roof extensometers

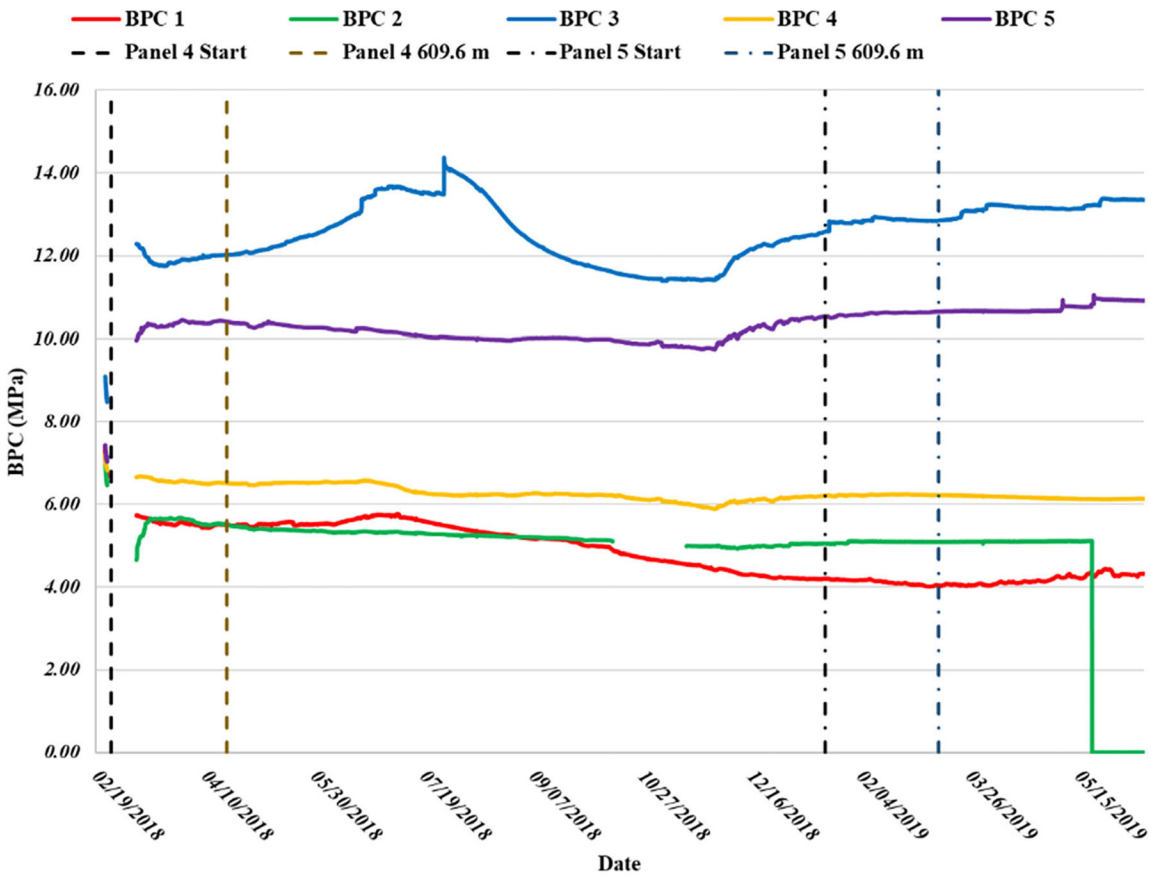

Fig. 8.

BPC results with panels 4 and 5 beginning and first 609.6 m of each panel notated

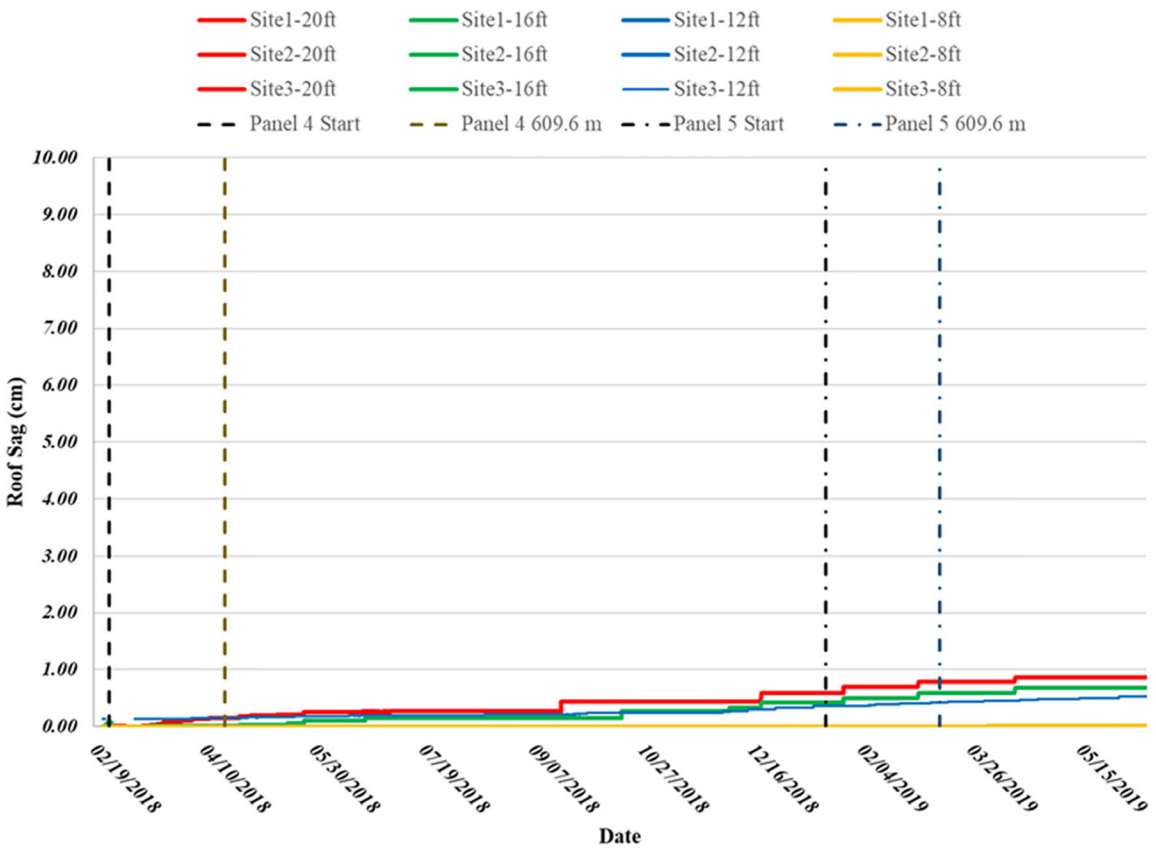

Fig. 9.
Roof extensometer data for the three sites

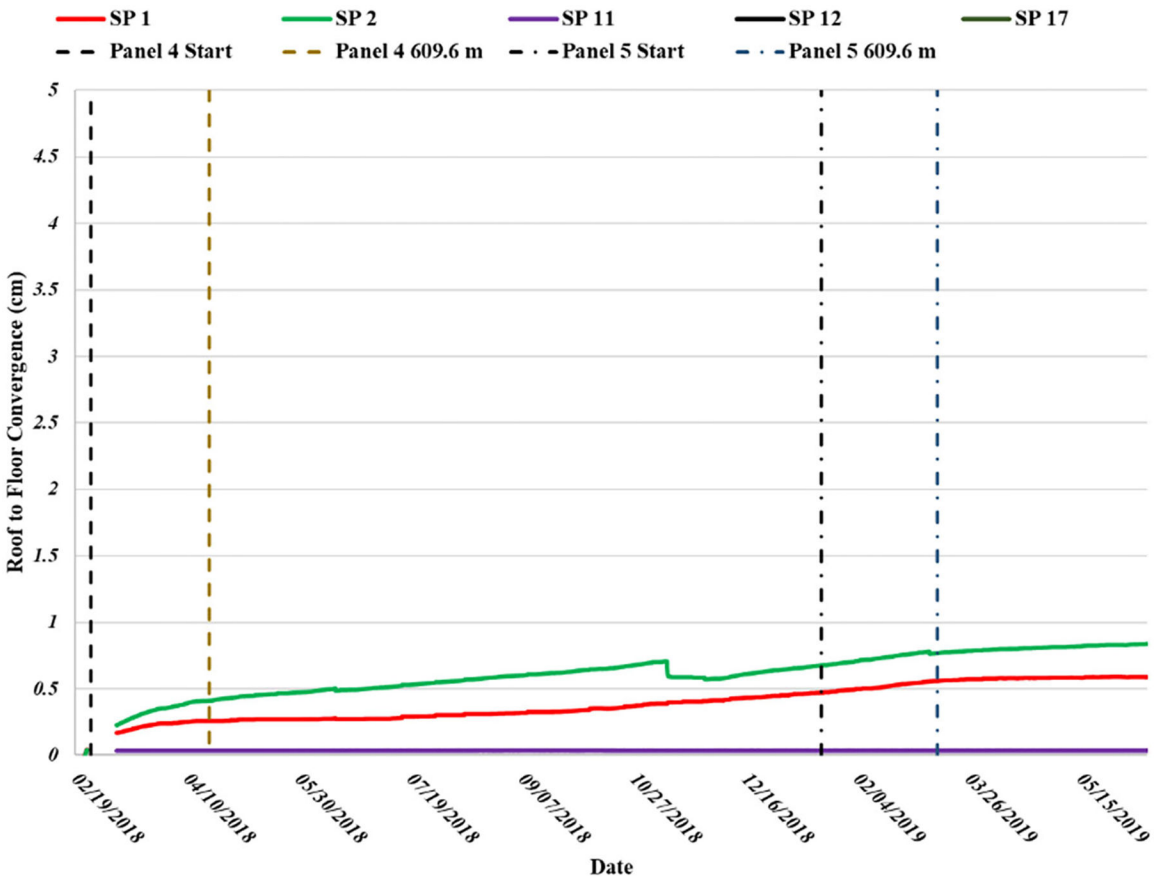

Fig. 10.
Convergence of the pumpable cribs during the monitoring period

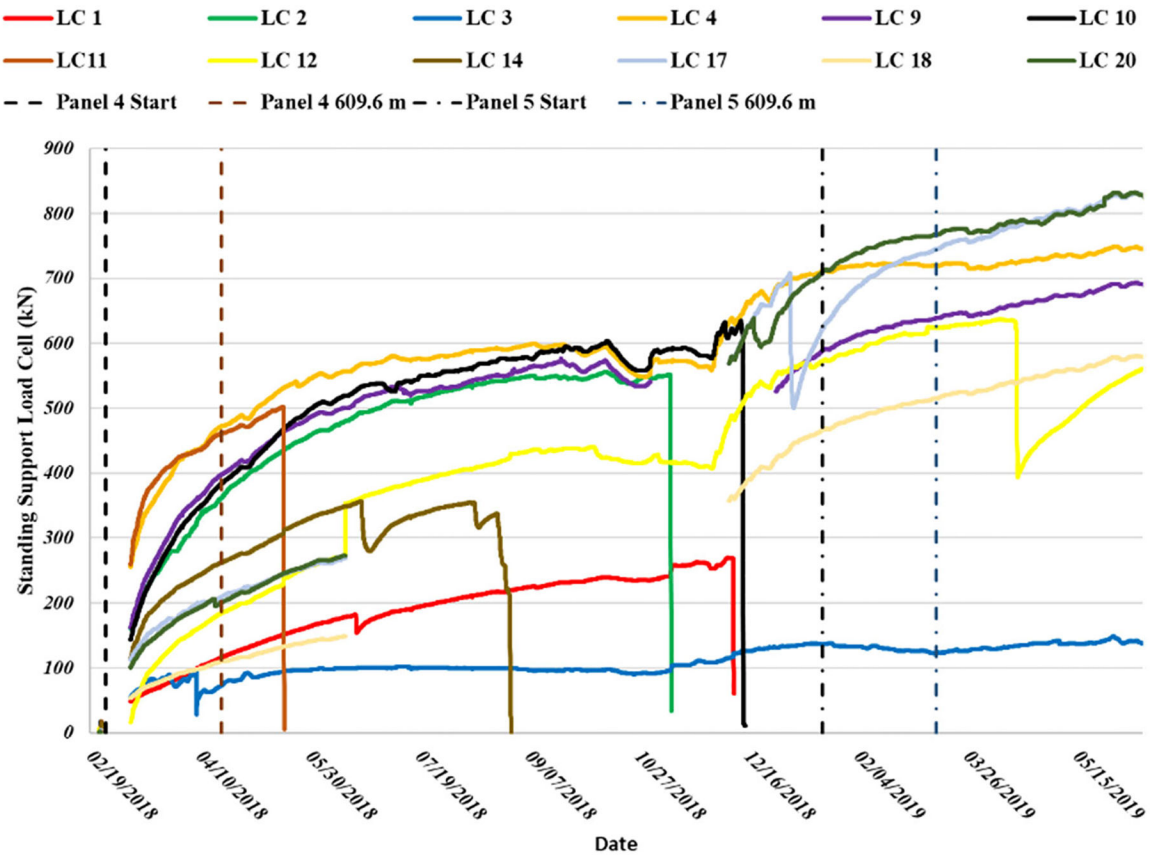

Fig. 11.
Standing support load cell data during the extraction of panels 4 and 5

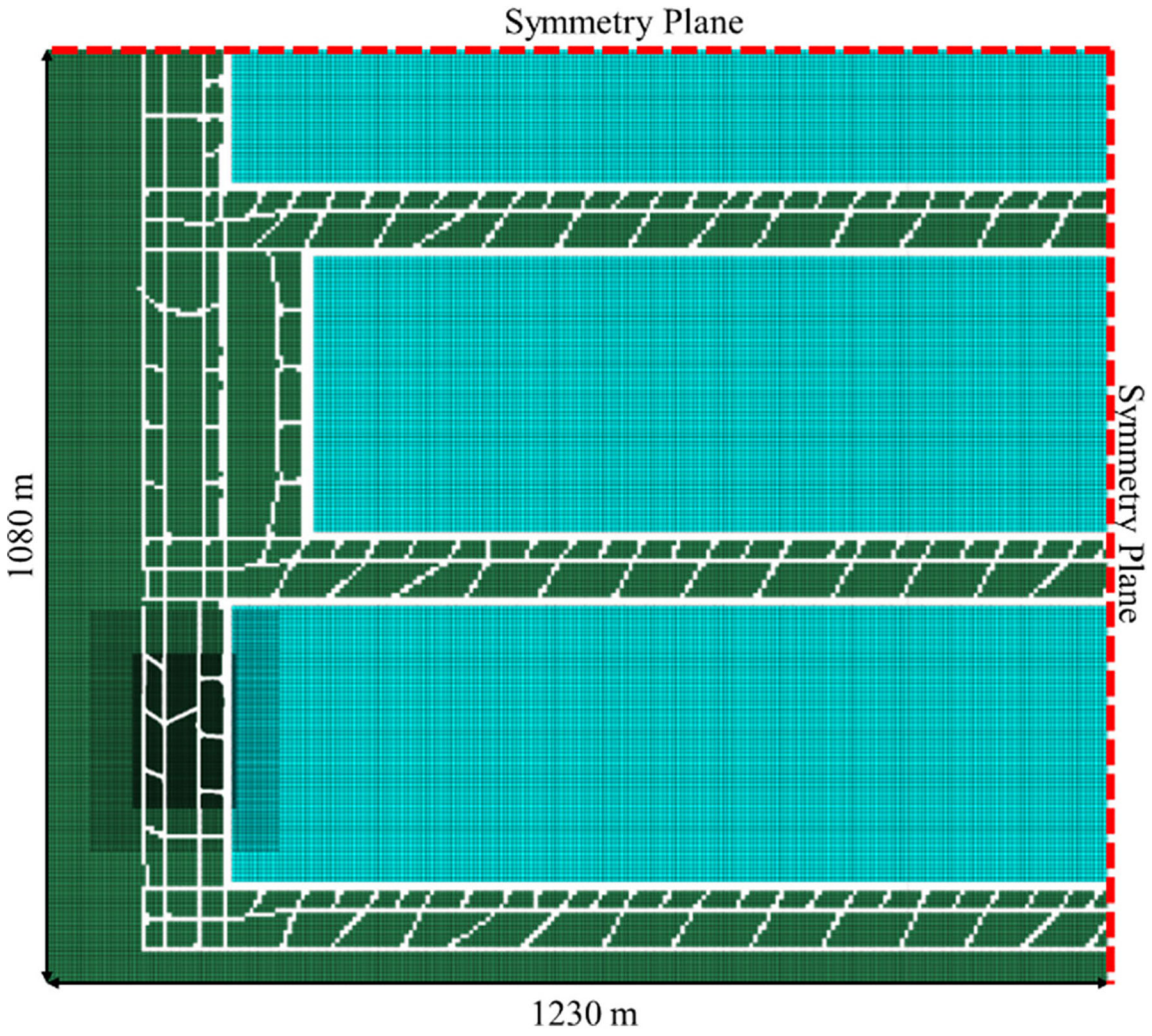

Fig. 12.
Plan view of the modeled area showing the increased zone density area of interest

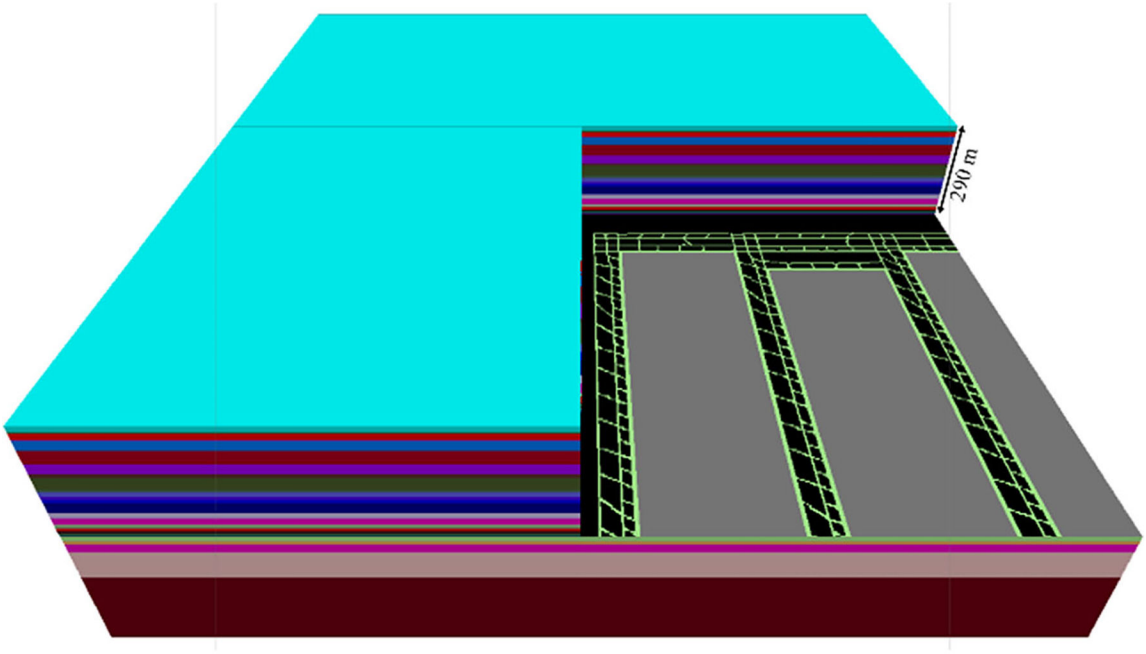

Fig. 13.
Image of the modeled geometry and overburden geological sequence

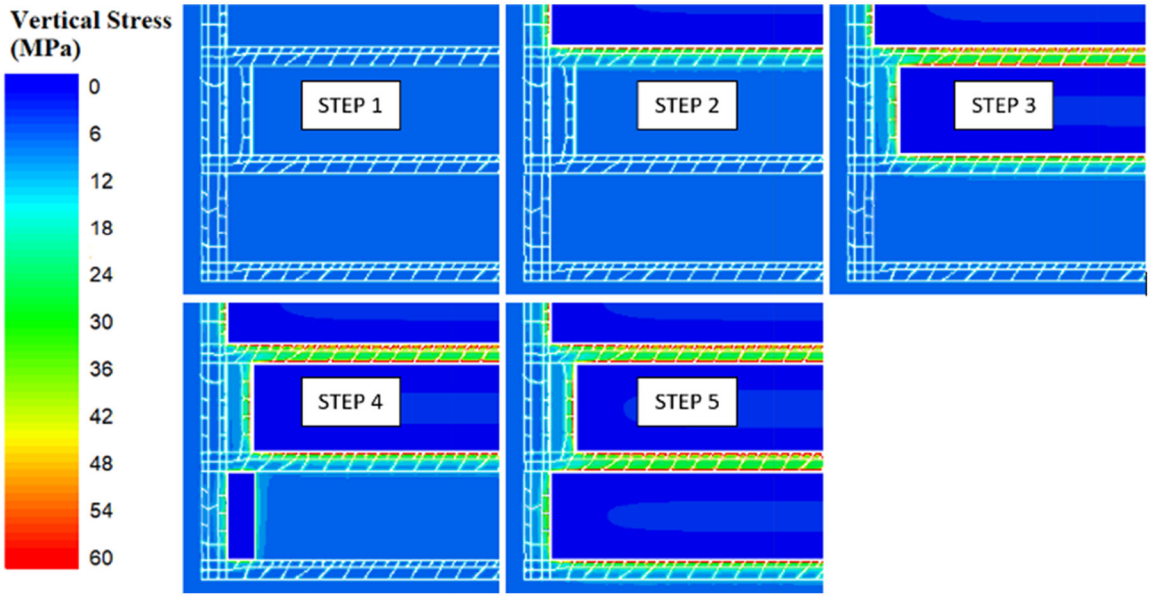

Fig. 14.
Global view of the vertical stress results for the five steps modeled

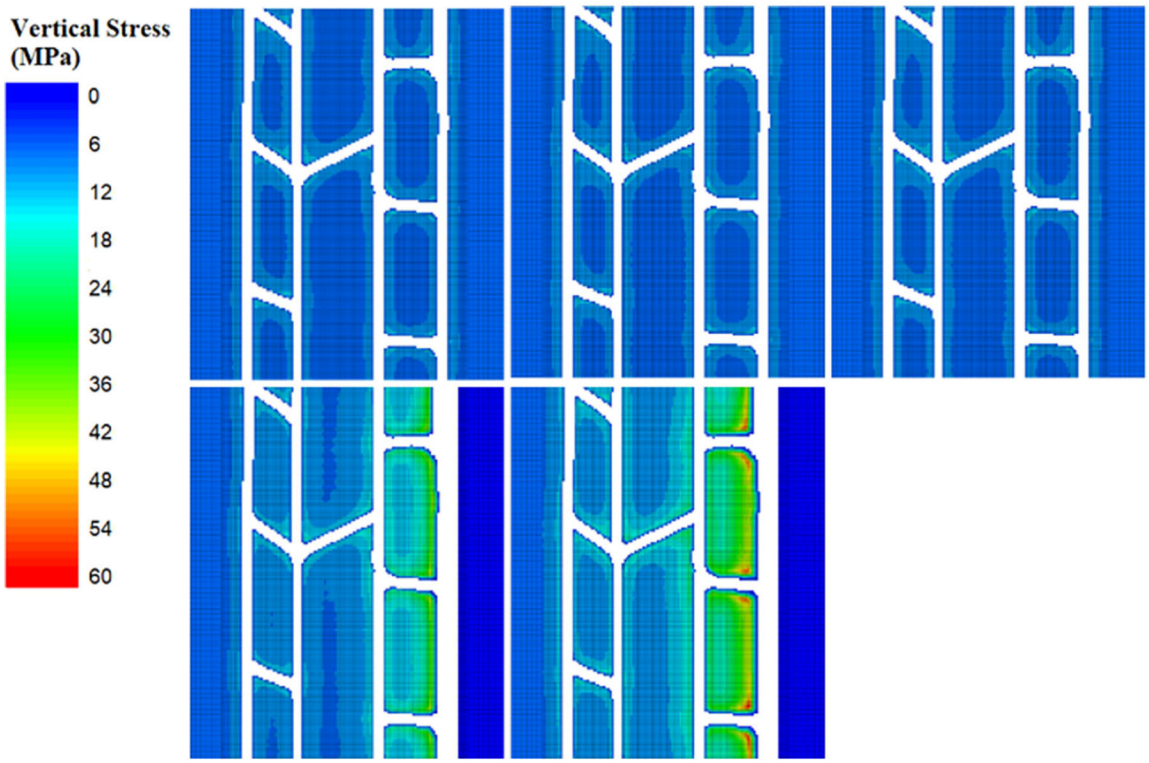

Fig. 15.
Local view of the vertical stress results around the instrumentation area for the five steps modeled

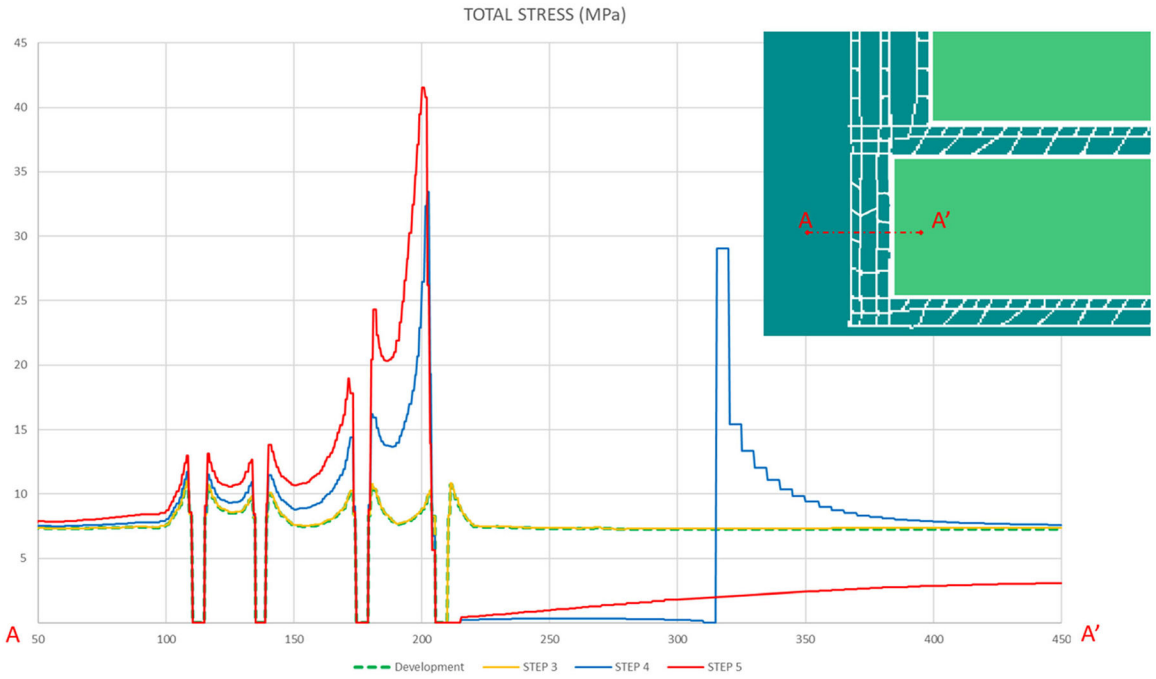

Fig. 16.
Bleeder vertical stresses for the five modeled mining steps on cross-section A-A'

Table 1

Modeled stress change between steps 3, 4, and 5

	Stress change (MPa)		
	Step 4–3	**Step 5–3**	**Step 5–4**
BPC-	0.7	2.0	1.3
BPC-2	1.4	3.5	2.1
BPC-3	2.2	5.4	3.1
BPC-4	2.9	3.0	0.1
BPC-5	6.0	13.0	7.1

Table 2

Modeled stress change compared to measurement for BPC-3 and BPC-5

	First 100 m		Highest during panel 4 retreat	
	Measured	**Model**	**Measured**	**Model**
BPC-3	3.4	2.2	6.9	5.4
BPC-5	3.4	6.0	3.4	13